Materials and Design 45 (2013) 52–55

Contents lists available at SciVerse ScienceDirect

Materials and Design

journal homepage: www.elsevier.com/locate/matdes

Short Communication

Effects of pore size on the mechanical properties of three-dimensionally ordered macroporous nickel

Zhenyu Li [a], Lili Yang [b], Yang Li [a], Yongning Yang [a], Changhai Zhou [a], Yanbo Ding [c], Jiupeng Zhao [c], Yao Li [a,*]

[a] Center for Composite Materials and Structure, Harbin Institute of Technology, Harbin 150001, China
[b] School of Transportation Science and Engineering, Harbin Institute of Technology, Harbin 150090, China
[c] School of Chemical Engineering and Technology, Harbin Institute of Technology, Harbin 150001, China

ARTICLE INFO

Article history:
Received 9 July 2012
Accepted 5 September 2012
Available online 12 September 2012

ABSTRACT

The mechanical properties of three-dimensionally ordered macroporous (3DOM) nickel with pore sizes between 312 and 1200 nm are explored under nanoindentation and microhardness tester. This paper demonstrates that the hardness and elastic modulus of 3DOM Ni increase as the pore size decreases. The phenomenon that "smaller is stronger" is mainly due to the combined effects of sharing the load with more and smaller pore cells, the decrease of the moment upon the small pore wall and larger surface area to volume ratio. The deformation process of 3DOM Ni is pore wall "fracture-dominated" under nanoindentation while "bending-dominated" under microhardness tester. The results demonstrate how pore size control at the microstructural scale can tailor hardness and elastic modulus and hold great potential for the design and application of new 3DOM materials and devices.

1. Introduction

Over the past several decades, three-dimensional ordered macroporous (3-DOM) materials have stimulated great interest as their promising applications in separation science, solar energy conversion, catalysis, nanoelectronics, magnetic storage devices, chemical sensors, and particularly photonic crystals [1–3]. To operate devices from 3DOM, mechanical properties of 3DOM are important for the functionality and reliability of 3DOM device. According to current theory models, the mechanical properties of porous materials can be demonstrated by scaling equations with the porosity or relative density of the porous materials as the dominating parameter, implying that the strength of 3DOM materials decreases with increasing porosity, and the mechanical properties such as the yield strength and hardness are assumed to be pore size-independent [4,5]. However, recent nanomechanical measurements have revealed that microstructures such as the ligament-size and the morphology of the pore walls have affected their mechanical properties. The yield strength of nanoporous gold increases as the ligament diameter decreases [6]. The strength of anodic aluminum oxide structures increases significantly with the regularity of their pore-channel arrangement, and wall thickness can govern the compressive strength of the micropillars [7,8]. Previous experimental studies on mechanical behavior of 3DOM have focused on indentation deformation behavior and mechanically responsive in filling mesopores with different secondary phase using depth-sensing indentation, through optimization of the synthesis of 3DOM C, the mechanical stability could be improved further [9,10]. However, the correlation between the pore cell geometry and mechanical properties has been much less studied and poorly understood.

The 3DOM Ni to be studied in this paper possess large-area structures and well-defined pore size, holding promising potential as battery electrodes, thermal emitters and photovoltaic devices [11,12]. Recently we reported the mechanical properties of 3DOM Ni using nanoindentation and found 3DOM nickel possessed excellent mechanical properties [13]. 3DOM Ni thus provides a model for studying the effects of pore size on the mechanical properties of 3DOM materials. This paper presents a study on the mechanical properties of 3DOM Ni with varying pore sizes using nanoindentation and microhardness tester. 3DOM Ni show mutable mechanical properties by manipulating the pore size. The phenomenon that "smaller is stronger" and the deformation process under indentation were investigated.

2. Experimental details

3DOM Ni samples, all with a theoretical porosities of 0.74, but with different pore sizes (312,375,572,900 and 1200 nm), were fabricated by colloidal crystal template-assisted electrodeposition method as described in detail in our previous papers [13,14]. Briefly, polystyrene opal templates with different diameters (312,375,620,900 and 1200 nm) were formed on nickel alloy

* Corresponding author. Tel./fax: +86 451 86403767.
E-mail address: yaoli@hit.edu.cn (Y. Li).

0261-3069/$ - see front matter © 2012 Elsevier Ltd. All rights reserved.
http://dx.doi.org/10.1016/j.matdes.2012.09.009

substrates. Then, Ni was infiltrated into templates by electrodeposition and 3DOM Ni was obtained by removing of polystyrene opal templates. The thickness of 3DOM was about 20 μm controlled by the electrodeposition time. The samples were tested using nanoindentation with a Berkovich diamond indenter (Hysitron Inc., TriboIndenter) and five experiments were conducted for each sample to determine average value of the mechanical parameters. The mechanical properties such as hardness and elastic modulus were calculated using the Oliver–Pharr method [15]:

$$H = \frac{P_{\max}}{A} \tag{1}$$

$$A = 24.5h_c^2 \tag{2}$$

$$\frac{1}{E_r} = \frac{1-\upsilon^2}{E} + \frac{1-\upsilon_i^2}{E_i} \tag{3}$$

where $P_{\max}$ is the peak load, A is the contact area, h_c is the contact depth, E and υ are the elastic modulus and poisson's ratio of the samples, and E_i and υ_i are the elastic modulus and poisson's ratio of the indenter, respectively. According to the standard of ISO 6507-1:2005 [16], the microhardness of 3DOM Ni was determined as the average of 10 measurements per-sample using a HVS-1000 type microhardness tester with a load of 50 g. The morphology and the residual indentation were characterized by scanning electron microscopy (SEM).

3. Results and discussion

The maximum loads (5 and 9 mN) are applied using nanoindentation. Fig. 1a shows the representative nanoindentation load–displacement (P–h) curves obtained from different 3DOM Ni samples, with pore size (312, 375, 620, 900 and 1200 nm). In general, with pore sizes decreasing, the shift of the P–h curves toward lower displacement values indicates that the strength of 3DOM Ni increases under the same loads (5 or 9 mN). 3DOM with smaller pore size can sustain relatively high loads at the same corresponding indentation depths and undergo more elastic recovery. Based on the load–displacement curve, the paper calculated the effective indentation hardness and elastic modulus of different 3DOM structures by the Oliver–Pharr method as a function of pore size, as shown in Fig. 1b and c, respective [15]. Errors of the mechanical properties measurement can come from the indentation position on pore or cell wall as well as the load and displacement measurements (see error bars in Fig. 1). The calculated results prove unambiguously that the hardness of 3DOM Ni is strongly size dependent, increasing from 85.54 to 717.75 MPa as the diameter decreased from 1200 down to 312 nm under 9 mN load, while from 88.11 to 797.42 MPa under 5 mN load. The highest hardness of 3DOM Ni is about nine times higher than its counterparts. Likewise, similar trends are observed in the elastic modulus, increasing from 1.55 to 8.13 GPa as the pore size decreases under 9 mN load, while from 1.75 to 9.57 GPa under 5 mN load. As aforementioned, the synthesis of these 3DOM Ni are not different from the porosities intended to be kept as constant (0.74) in this study, which indicates that the mechanical properties are affected by the pore size variations in the 3DOM. The results demonstrate the trend that "smaller is stronger" in 3DOM.

To further probe the mechanism for the pore size dependence in the mechanical properties, the dependence of the maximum displacement and the residual displacement as a function of pore size have been examined. Fig. 2a displays the maximum displacement increases with increasing pore size, and the maximum displacement of 3DOM Ni with the biggest pore size is approximately 2.5 times bigger than the smallest one. Fig. 2b reveals that the residual displacement increases as the pore size decreasing under the same load. For a 3DOM Ni with small pore size, enhancing the number of pore cells under the indenter that can activate band formation and increasing the elastic constraint. The load can be distributed over more pore cells and causes more resistance toward cell deformation during indentation. The load on the single pore decreases as

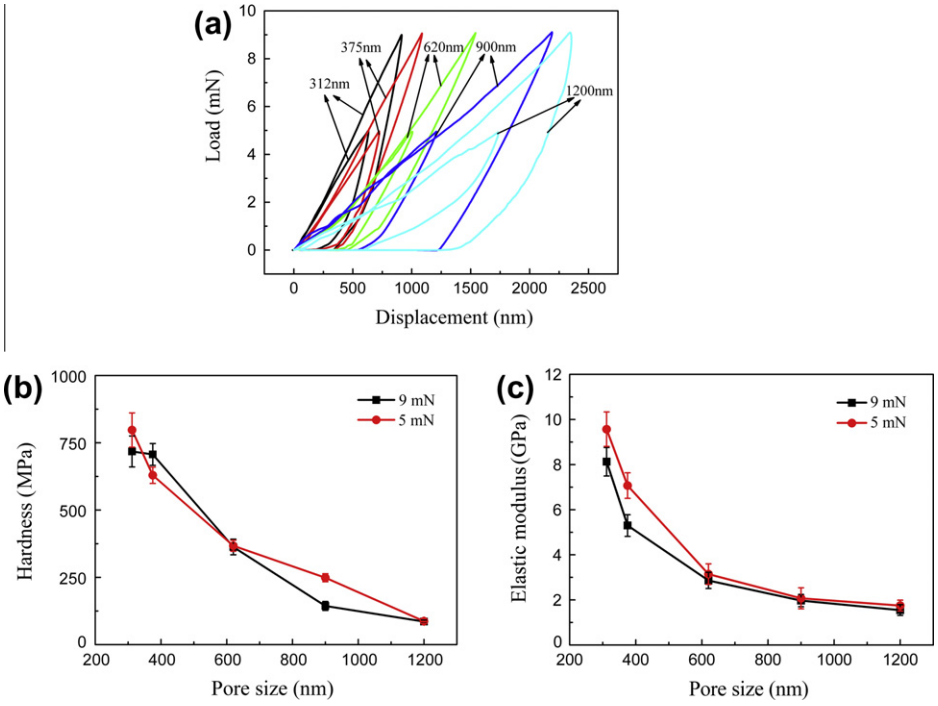

Fig. 1. (a) The representative load–displacement curves as a function of pore size with maximum loads of 5 and 9 mN. (b) The hardness and (c) the elastic modulus of 3DOM Ni with different pore sizes under the two loads.

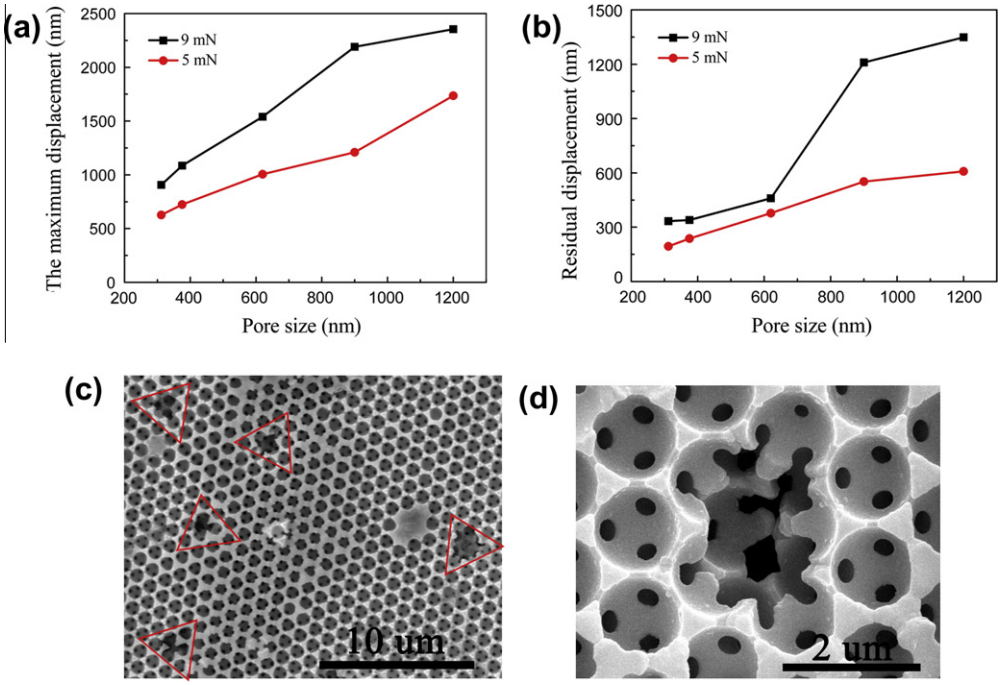

Fig. 2. (a) The maximum displacement and (b) the residual displacement at the load 5 mN and 9 mN; (c) and (d) SEM of the residual nanoindentation impression of 3DOM Ni (with pore size 1200 nm) under 5 mN load.

well due to more pore share the load. This causes an increase in the indentation strength with decreasing pore size. Additional, the pore size-dependent mechanical properties can also result from the decrease of the moment upon the small pore wall. Xu has reported that the moment upon the cell wall decreases as the decrease of the average cell size of Mg alloy foams [17]. The results indicate that the greater aspect ratio of the pore walls in the smaller pore size 3DOM Ni can suffer larger load. Finally, all these demonstrate that controlling the pore size can improve the strength of the 3DOM by sharing the load with more and smaller pore cells.

As can be seen from Fig. 2c and d, the residual indentation reveals that the deformation is predominately confined to the area under the indenter and the deformation under the nanoindentation in 3DOM Ni is fracture-dominated. As the load rises up, the first layer pores wall will bend and fracture. Then the load increases and the indenter reach the next pore layer and the process is repeated again.

To extend our study on the phenomenon "smaller is stronger" in 3DOM, the microhardness has been tested. The variation of microhardness as a function of pore size is plotted in Fig. 3a. The size dependence following the same trend as the nanoindentation experimentally is found. The microhardness increases from 230.67 HV to 358.03 HV as the pore sizes decrease from 1200 to 312 nm, and the microhardness then varies sharply at the small size. The microhardness of the smallest pore size sample is 358.03 HV, close to the microhardness of the macrograin-Ni fabricated by the same methods [18]. Fig. 3b shows the details of the deformation. Fig. 3b indicates that the deformation mechanism of indentation are more "bending-dominated", including the elastic deformation of cell-wall bending, pore collapse, localized densification and compaction. The deformation closer to the indentation center corresponds to severe densification and compaction of the 3DOM Ni structure, whereas that further away from the center corresponds to bending and tilting of the pore walls instead of full collapse of the 3DOM structure.

The observed pore size effect on mechanical properties of 3DOM may also be related to the enhancement in their large surface area to volume ratio, Lu have reported the theoretical results show that the Young's modulus of the nanoporous materials increases as the strut size decreases due to surface effects [19].

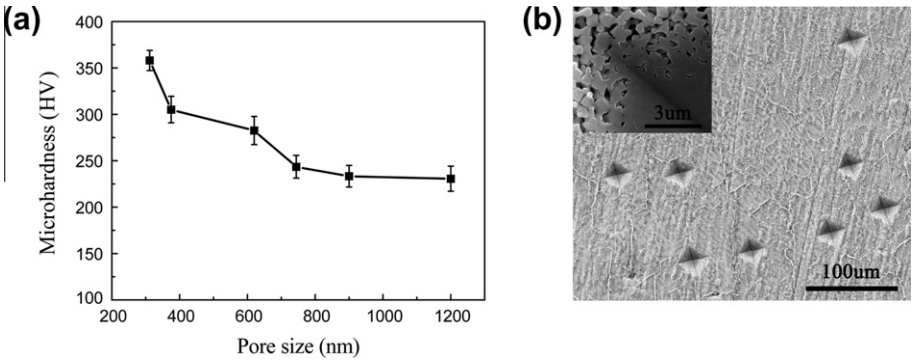

Fig. 3. (a) The microhardness of the 3DOM Ni with different pore sizes and (b) SEM of residual indentation impression of 3DOM Ni with pore size 1200 nm under 0.49 N load.

Ni and Ag nanowires, which closely resemble the pore ligaments (or struts) in 3DOM materials, have shown a similar phenomenon that "smaller is stronger" under tension or compression as a result of their large surface area to volume ratio, mainly surface elasticity [20,21]. Wang has found that yield strength and tensile strength increased as the NW diameter decreased due to the stiffening size effect in Young's modulus and the surface effect [21]. The present results illustrate that the pore size of the 3DOM is an important factor governing the mechanical strength of 3DOM. Unlike traditional porous materials, the pore geometry of the 3DOM can be rationally designed. With the present technique to control the pore size by colloidal crystal template-assisted method, other properties of 3DOM structures can be investigated systematically as a function of their pore size.

4. Conclusions

In summary, this paper has investigated how the mechanical properties of three-dimensionally ordered macroporous Ni depend on pore size using nanoindentation and microhardness tester. The deformation mechanism of 3DOM Ni using nanoindentation is close to pore wall "fracture-dominated" while microhardness tests are more "bending-dominated". The study has shown that 3DOM Ni with small pore size can have enhanced hardness and modulus. This enhancement may result from sharing the load with more and smaller pores, the decrease of the moment upon the pore wall and large surface area to volume ratio. These results demonstrate that the mechanical properties of 3DOM Ni can be uniquely tailored by manipulating the pore size. The phenomenon "smaller is stronger" in 3DOM indicate that the future 3DOM materials may be further optimized to design more robust 3DOM devices for engineering applications.

Acknowledgments

We thank National Natural Science Foundation of China (Nos. 51010005, 90916020, 51174063 and 51102068), the Program for New Century Excellent Talents in University (NCET-08-0168), and the Fundamental Research Funds for the Central Universities (HIT.ICRST.2010001) and Sino-German joint Project (GZ550).

References

[1] Fleming JG, Lin SY, El-Kady I, Biswas R, Ho KM. All-metallic three-dimensional photonic crystals with a large infrared bandgap. Nature 2002;417:52–5.
[2] Velev OD, Jede TA, Lobo RF, Lenhoff AM. Porous silica via colloidal crystallization. Nature 1997;389:447–8.
[3] Galisteo-López JF, Ibisate M, Sapienza R, Froufe-Pérez LS, Blanco Á, López C. Self-assembled photonic structures. Adv Mater 2011;23:30–69.
[4] Gibson LJ, Ashby MF. Cellular solids: structure and properties. 2nd. Cambridge, UK: Cambridge University Press; 1997.
[5] Rice RW. Evaluation and extension of physical property–porosity models based on minimum solid area. J Mater Sci 1996;31:102–18.
[6] Biener J, Hodge AM, Hayes JR, Volkert, Zepeda-Ruiz LA, Hamza AV, et al. Size effects on the mechanical behavior of nanoporous Au. Nano Lett 2006;6:2379–82.
[7] Ng KY, Ngan AHW. Effects of pore-channel ordering on the mechanical properties of anodic aluminum oxide nano-honeycombs. Scripta Mater 2012;66:439–42.
[8] Fan HD, Li ZH, Huang MS. Size effect on the compressive strength of hollow micropillars governed by wall thickness. Scripta Mater 2012;67:225–8.
[9] Toivola Y, Stein A, Cook RF. Depth-sensing indentation response of ordered silica foam. J Mater Res 2004;19:260–71.
[10] Wang Z, Li F, Ergang NS, Stein A. Effects of hierarchical architecture on electronic and mechanical properties of nanocast monolithic porous carbons and carbon–carbon nanocomposites. Chem Mater 2006;18:5543–53.
[11] Zhang HG, Yu XD, Braun PV. Three-dimensional bicontinuous ultrafast-charge and-discharge bulk battery electrode. Nat Nanotechnol 2011;6:277–81.
[12] Zhang HG, Braun PV. Three-dimensional metal scaffold supported bicontinuous silicon battery anodes. Nano Lett 2012;6:2778–83.
[13] Li Y, Ma B, Zhao JP, Xin WH, Wang XJ. Excellent mechanical properties of three-dimensionally ordered macroporous nickel photonic crystals. J Alloy Compd 2011;509:290–3.
[14] Meng XD, Al-Salman R, Zhao JP, Borissenk N, Li Y, Endres F. Electrodeposition of 3D ordered macroporous germanium from ionic liquids: a feasible method to make photonic crystals with a high dielectric constant. Angew Chem Int Edit 2009;15:2703–7.
[15] Oliver WC, Pharr GM. An improved technique for determining hardness and elastic modulus using load and displacement sensing indentation experiments. J Mater Res 1992;7:1564–83.
[16] ISO 6507–1:2005. Metallic materials–Vickers hardness test – Part 1: Test method. ISO; 2005.
[17] Xu ZG, Fu JW, Luo TJ, Yang YS. Effects of cell size on quasi-static compressive properties of Mg alloy foams. Mater Des 2012;34:40–4.
[18] Kang JX, Zhao WZ, Zhang GF. Influence of electrodeposition parameters on the deposition rate and microhardness of nanocrystalline Ni coatings. Surf Coat Technol 2009;203:1815–8.
[19] Xia R, Li XD, Qin QH, Liu JL, Feng XQ. Surface effects on the mechanical properties of nanoporous materials. Nanotechnology 2011;22:265714.
[20] Sansoz F, Dupont V. Nanoindentation and plasticity in nanocrystalline Ni nanowires: a case study in size effect mitigation. Scripta Mater 2010;63:1136–9.
[21] Zhu Y, Qin QQ, Xu F, Fan FR, Ding Y, Zhang T, et al. Size effects on elasticity, yielding, and fracture of silver nanowires: in situ experiments. Phys Rev B 2012;85:045443.